NMO ellipse for a stratified medium with laterally varying velocity

Mamoru Takanashi[1,2] & Ilya Tsvankin[1]

[1] *Center for Wave Phenomena, Geophysics Department, Colorado School of Mines, Golden, Colorado 80401*
[2] *Japan Oil, Gas and Metals National Corporation, Chiba, Japan*

ABSTRACT

Analysis of azimuthally varying normal-moveout velocity (i.e., of the NMO ellipse) is often performed under the assumption that the overburden is laterally homogeneous on the scale of spreadlength. However, small-scale lateral heterogeneity can significantly influence both effective and interval NMO ellipses. Here, we derive an analytic expression for the NMO ellipse in a horizontally layered anisotropic medium with lateral velocity variation. The equation demonstrates that the distortion of the effective NMO ellipse is caused primarily by the quadratic lateral variation of the vertical velocity, which can be represented through the curvature of the vertical traveltime surface. The magnitude of the distortion rapidly increases with the distance between the target and a laterally heterogeneous layer in the overburden. Application of Dix-type differentiation without correcting for the lateral velocity variation can strongly amplify the false elongation or compression of the effective NMO ellipse. Synthetic tests for layered isotropic and HTI (transversely isotropic with a horizontal symmetric axis) media confirm that the presented equation closely approximates the influence of a thin, weakly heterogeneous layer in the overburden on the NMO ellipse. Hence, our results provide the basis for moveout analysis of wide-azimuth data from stratified media with mild lateral velocity variation.

Key words: NMO ellipse, lateral heterogeneity, azimuthal anisotropy, wide-azimuth, generalized Dix differentiation

1 INTRODUCTION

Azimuthal variation of NMO velocity for pure (non-converted) modes is typically elliptical, even if the medium is strongly anisotropic and moderately heterogeneous (Grechka and Tsvankin, 1998). Even in the presence of nonhyperbolic moveout, the NMO ellipse controls the most stable, near-offset portion of the moveout function (Tsvankin, 2005). The elliptical dependence of NMO velocity provides the basis for moveout analysis and stacking of wide-azimuth data (e.g., Grechka and Tsvankin, 1999; Jenner et al., 2001; Tsvankin, 2005). Interval NMO ellipses can be obtained from the generalized Dix equation, which operates with the effective NMO ellipses for the top and bottom of the target layer (Grechka et al., 1999).

Time-domain analysis of the NMO ellipse is typically performed under the assumption that the overburden is laterally homogeneous on the scale of spreadlength. However, case studies indicate that lateral heterogeneity (e.g., small-scale velocity lenses, such as channels and reefs) can seriously distort the NMO ellipse and its interpretation in terms of fracture parameters (Luo et al., 2007; Jenner, 2009). Jenner (2010) shows that interval NMO ellipses computed from the Dix-type method are more influenced by the lateral variation of the vertical velocity than by laterally changing anisotropy parameters.

Grechka and Tsvankin (1999) derive an analytic expression designed to remove the influence of weak lateral velocity variation on the NMO ellipse in a stack of horizontal layers. They show that the correction term depends primarily on the second horizontal derivatives of the vertical velocity and present a processing flow for moveout inversion of wide-azimuth data that includes 3D semblance analysis, correction for lateral velocity variation, and the generalized Dix differentiation. However, their equation is not suited for removing the distor-

tions caused by thin, laterally heterogeneous (LH) beds in a multilayered medium. Blias (2009) and Takanashi and Tsvankin (2010) show that the influence of a velocity lens on NMO velocity in 2D models typically increases with distance between the lens and the target reflector.

Here, we analyze the influence of a thin, laterally heterogeneous layer in the overburden on the effective and interval NMO ellipses. We derive an expression for the effective NMO ellipse in a horizontally layered LH model by generalizing the equation of Grechka and Tsvankin (1999). The analytic results show that the LH-induced distortion in the NMO ellipse increases monotonically with the target depth. The error in the effective ellipse is amplified by the generalized Dix differentiation used to obtain the interval NMO ellipse. Correction of the NMO ellipse for lateral heterogeneity requires estimating a circular (isotropic) approximation of the interval NMO ellipse in each layer, as well as the second horizontal derivatives of the vertical traveltime for the LH layer(s). Synthetic tests confirm that our formalism accurately describes the influence of a thin, weakly heterogeneous layer in the overburden on the NMO ellipse.

2 NMO ELLIPSE IN STRATIFIED LH MEDIA

To study the influence of a thin laterally heterogeneous layer on the effective and interval NMO ellipses, we generalize the equation introduced by Grechka and Tsvankin (1999). The hyperbolic moveout equation for wide-azimuth data has the form (Grechka and Tsvankin, 1998):

$$t^2(h,\,\alpha) = t_0^2 + \frac{x^2}{V_{\rm nmo}^2(\alpha)}\,, \tag{1}$$

where h is the half-offset, α is the azimuth of the CMP line, t_0 is the zero-offset traveltime, and $V_{\rm nmo}(\alpha)$ is the NMO velocity given by

$$V_{\rm nmo}^{-2}(\alpha) = W_{11}\cos^2\alpha + 2W_{12}\sin\alpha\cos\alpha + W_{22}\sin^2\alpha\,. \tag{2}$$

The symmetric 2×2 matrix W_{ij} depends on the second spatial derivatives of the one-way traveltime τ from the zero-offset reflection point to the surface location $[x_1,\,x_2]$:

$$W_{ij} = \tau_0\,\frac{\partial^2\tau}{\partial x_i\,\partial x_j}\bigg|_{\mathbf{x}=\mathbf{x}_{\rm CMP}} \quad (i,\,j=1,\,2)\,; \tag{3}$$

τ_0 is the one-way zero-offset time.

Equation 2 can be simplified by aligning the horizontal coordinate axes with the eigenvectors of the matrix W_{ij} (Grechka and Tsvankin, 1998):

$$V_{\rm nmo}^{-2}(\alpha) = \lambda_1\cos^2(\alpha-\beta) + \lambda_2\sin^2(\alpha-\beta)\,, \tag{4}$$

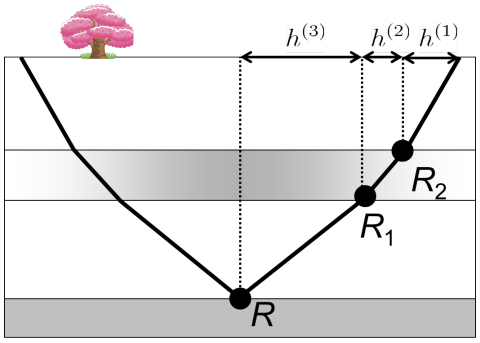

Figure 1. Reflection raypath through a horizontal three-layer model. $h = h^{(1)} + h^{(2)} + h^{(3)}$ is the half offset, R is the reflection point for the unperturbed ray, and R_1 and R_2 are the intersection points with layer boundaries. Following Grechka and Tsvankin (1999), the raypath perturbation caused by weak lateral heterogeneity is assumed to be negligible, and the ray is confined to the vertical plane. Only in the second layer is laterally heterogeneous.

where λ_1 and λ_2 are the eigenvalues of the matrix W_{ij}, and β is the angle between the eigenvector corresponding to λ_1 and the x_1-axis.

In the special case of a horizontal, anisotropic layer with a horizontal symmetry plane, the influence of weak LH is represented by (Grechka and Tsvankin, 1999)

$$W_{ij}^{\rm hom} = W_{ij}^{\rm het} - \frac{\tau_0}{3}\,\frac{\partial^2\tau_0}{\partial y_i\,\partial y_j}\bigg|_{\mathbf{y}=\mathbf{y}_{\rm CMP}}\,,\ (i,\,j=1,\,2)\,, \tag{5}$$

where $W_{ij}^{\rm het}$ is the NMO ellipse in the presence of lateral velocity variation, $W_{ij}^{\rm hom}$ is the NMO ellipse for the reference homogeneous model which has the same medium parameters as those at the CMP location, and $\tau_0 = \tau_0(\mathbf{y})$ is the one-way zero-offset traveltime at the CMP location $\mathbf{y}_{\rm CMP}$. The absence of the first derivatives of τ_0 indicates that a constant lateral gradient does not distort the NMO ellipse, which is governed by quadratic lateral velocity variation.

To study the dependence of the NMO ellipse on the depth and thickness of an LH interval, we use a three-layer model where lateral velocity variation is confined to the second layer (Figure 1). We assume not only that lateral heterogeneity is weak and the horizontal plane is a plane of symmetry, but also that the medium is weakly anisotropic. The same assumptions were made by Grechka and Tsvankin (1999,Appendix B) in their derivation of the NMO ellipse for a model with two LH layers. Following their approach, we obtain the NMO ellipse for the reflection from the bottom of the three-layer model as:

$$W_{ij}^{\rm hom} = W_{ij}^{\rm het} - \frac{\tau_0\,D}{3}\,\frac{\partial^2\tau_{02}}{\partial y_i\,\partial y_j}\bigg|_{\mathbf{y}=\mathbf{y}_{\rm CMP}}\,,\ (i,\,j=1,2) \tag{6}$$

where

$$D = k^2 + 3k\,l + 3l^2, \tag{7}$$

$$k = \frac{\tau_{02}(V_{\rm cir}^{(2)})^2}{\tau_{01}(V_{\rm cir}^{(1)})^2 + \tau_{02}(V_{\rm cir}^{(2)})^2 + \tau_{03}(V_{\rm cir}^{(3)})^2}\,, \tag{8}$$

and

$$l = \frac{\tau_{03}(V_{\rm cir}^{(3)})^2}{\tau_{01}(V_{\rm cir}^{(1)})^2 + \tau_{02}(V_{\rm cir}^{(2)})^2 + \tau_{03}(V_{\rm cir}^{(3)})^2}\,. \tag{9}$$

Here, τ_{01}, τ_{02} and τ_{03} are the vertical one-way interval traveltimes for the first, second, and third layers, respectively, and $V_{\rm cir}^{(1,2,3)}$ are the best-fit circles approximating the interval NMO ellipses for each layer (Grechka and Tsvankin, 1999):

$$V_{\rm cir}^{-2} = \frac{1}{2\pi}\int_0^{2\pi} V_{\rm nmo}^{-2}(\alpha)d\alpha = \frac{W_{11}^{\rm hom} + W_{22}^{\rm hom}}{2}$$

$$\approx \frac{W_{11}^{\rm het} + W_{22}^{\rm het}}{2}. \tag{10}$$

The coefficient D is determined by the parameters k and l, which can be obtained from interval moveout analysis using the Dix-type method. If the vertical velocity variation is weak, k and l are approximately equal to the relative thicknesses of the second and third layers, respectively.

When $l = 0$, the model includes just an LH layer overlaid by a homogeneous layer, and the term D reduces to k^2. This result, obtained by Grechka and Tsvankin (1999), indicates that the influence of a thin LH layer located immediately above the target reflector is insignificant. Indeed, when the relative thickness of the LH layer is 0.1, the term D reduces to just 0.01 (equations 6 and 7 and Figure 2), compared to unity for a single LH layer (equation 5).

However, the influence of the LH layer rapidly increases with the thickness of the layer beneath it and reaches its maximum when the LH layer is located at the top of the model (the term D reaches 2.71 when $k = 0.1$ and $l = 0.9$). Indeed, the influence of a thin LH layer on the NMO ellipse is proportional to the squared relative thickness of the third (underlying) layer because $3l^2$ in equation 7 makes the primary contribution to D when $l \gg k$. Thus, the depth and thickness of the LH layer are key parameters responsible for the influence of lateral heterogeneity.

For a fixed depth of the LH layer, the influence of lateral heterogeneity increases with target depth not only because of a larger coefficient D, but also because of the increase in the total vertical traveltime τ_0 (equation 6). This conclusion is confirmed by the test in Figure 3. The NMO-velocity error monotonically increases with the depth of the target reflector and also with the velocity in the third (deepest) layer. Indeed, the correction term makes a more significant contribution to $W_{ij}^{\rm het}$ when $W_{ij}^{\rm hom}$ is small (i.e., the reference NMO velocity is high; equation 6).

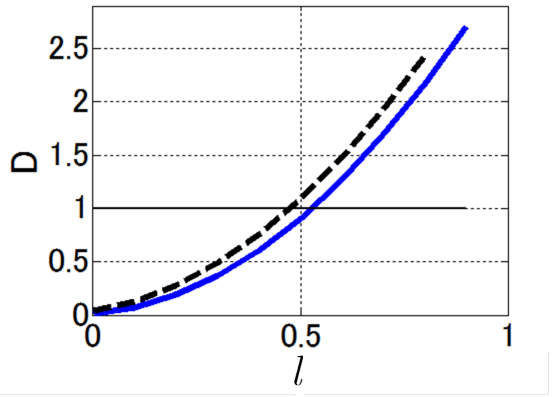

Figure 2. Coefficient D computed from equation 7 as a function of l for $k = 0.1$ (solid line) and $k = 0.2$ (dashed). D=1 (thin horizontal line) corresponds to a single LH layer.

In the linear approximation, the raypath perturbation caused by weak lateral heterogeneity can be ignored, which helps extend the derivation of Grechka and Tsvankin (1999,Appendix B) to an arbitrary number of LH layers. Equation 6 can be generalized for a stack of Nlayers (each layer can be LH) as:

$$W_{ij}^{\rm hom} = W_{ij}^{\rm het} - \sum_{m=1}^{N} \frac{\tau_0\, D_m}{3}\; \frac{\partial^2 \tau_{0m}}{\partial y_i\, \partial y_j}\bigg|_{\mathbf{y}=\mathbf{y}_{\rm CMP}}\,,$$

$$(i,\, j = 1,\, 2)\,, \tag{11}$$

where

$$D_m = k_m^2 + 3k_m\, l_m + 3l_m^2, \tag{12}$$

$$k_m = \frac{\tau_{0m}(V_{\rm cir}^{(m)})^2}{\sum_{r=1}^{N} \tau_{0r}(V_{\rm cir}^{(r)})^2}\,, \tag{13}$$

and

$$l_m = \frac{\sum_{r=m+1}^{N} \tau_{0r}(V_{\rm cir}^{(r)})^2}{\sum_{r=1}^{N} \tau_{0r}(V_{\rm cir}^{(r)})^2}\,. \tag{14}$$

If layer m is laterally homogeneous, the mth correction term goes to zero because $\tau_{0m} = $const. The correction term in equation 11 is obtained by adding the contributions of all LH layers. The coefficient D_m for each LH layer is determined by the coefficient k_m and l_m, which are computed from the best-fit interval NMO circles in all layers.

The exact reference interval NMO ellipse in the Nth layer can be found from the generalized Dix equation (Grechka et al., 1999):

$$\mathbf{W}_{n,\rm hom}^{-1} = \frac{t(N)\,\mathbf{W}_{\rm hom}^{-1}(N) - t(N-1)\mathbf{W}_{\rm hom}^{-1}(N-1)}{t(N) - t(N-1)}\,,$$

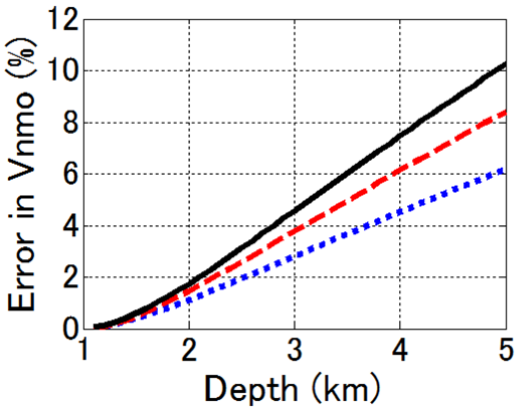

Figure 3. Error in the effective NMO velocity in the y_1-direction for a three-layer isotropic model where lateral heterogeneity is confined to the second layer. The horizontal axis is the depth of the target interface (the bottom of the third layer). The velocity at the CMP location ($y_1 = 0$ km) in the first and second layers is 3 km/s, and in the third layer 2 km/s (dotted line), 3 km/s (dashed) and 4 km/s (solid). The second (LH) layer is located at 1 km depth with thickness $z_2 = 0.2$ km and $\partial^2\tau_{02}/\partial y_1^2 = 0.02\,(\mathrm{s/km^2})$, which corresponds to a 10 ms perturbation of τ_{02} or a 13% velocity perturbation at $y_1 = \pm 1$ km. There is no linear lateral velocity variation in any layer.

(15)

where $\mathbf{W}_{\mathrm{hom}}(N)$ and $\mathbf{W}_{\mathrm{hom}}(N-1)$ describe the reference effective NMO ellipses for the top and bottom of the Nth layer, and $t(N)$ and $t(N-1)$ are the corresponding zero-offset traveltimes. When the target interval is located beneath the LH layer, the distortion in $\mathbf{W}_{\mathrm{het}}(N)$ is larger than that in $\mathbf{W}_{\mathrm{het}}(N-1)$ (see Figure 3). Hence, substitution of $\mathbf{W}_{\mathrm{het}}(N)$ and $\mathbf{W}_{\mathrm{het}}(N-1)$ for $\mathbf{W}_{\mathrm{hom}}(N)$ and $\mathbf{W}_{\mathrm{hom}}(N-1)$, respectively, causes distortions in the interval ellipse $\mathbf{W}_n$ obtained from equation 15. Although the difference in the correction term between $\mathbf{W}_{\mathrm{het}}(N)$ and $\mathbf{W}_{\mathrm{het}}(N-1)$ may be relatively small for a thin Nth layer, the LH-induced distortion is amplified by the Dix differentiation (Figure 4b). Clearly, $\mathbf{W}_{\mathrm{het}}(N)$ and $\mathbf{W}_{\mathrm{het}}(N-1)$ should be corrected for lateral heterogeneity before applying equation 15.

The correction term in equation 11 is determined by the total vertical traveltime, the coefficient D_m for the mth LH layer, and the second derivatives of the interval vertical traveltime $\partial^2\tau_{0m}/(\partial y_i\,\partial y_j)$. Whereas D_m can be approximately found in a relatively straightforward way, evaluating the second derivatives of τ_{0m} for field data generally requires spatial smoothing, as discussed by Grechka and Tsvankin (1999). One possible approach for estimating $\partial^2\tau_{0m}/(\partial y_i\,\partial y_j)$ is to measure the vertical traveltime distortion (i.e., pull-up or push-down time anomalies) on the near-offset stacked section and approximate the spatial traveltime variation by a quadratic function (curvature) of the horizontal coordinates. In a sequel paper (Takanashi and Tsvankin, 2011), we discuss evaluation of the traveltime curvature and estimation of laterally-varying distortions of NMO ellipses for models with a thin velocity lens.

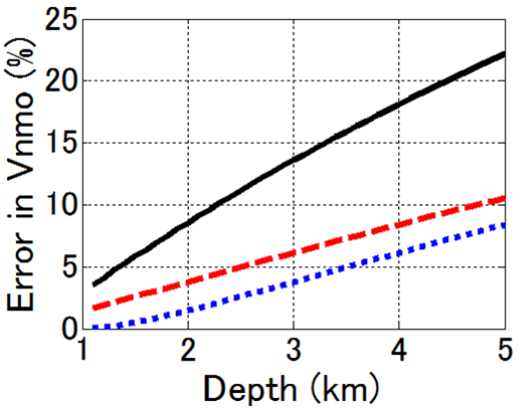

(a)

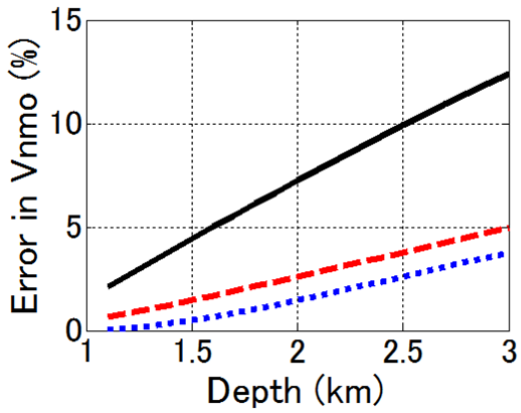

(b)

Figure 4. Error in the interval NMO velocity (solid line) in the bottom layer of the model from Figure 3. V_{nmo} is computed in the y_1-direction using equation 15. Errors in the effective NMO velocities for the top (dotted) and bottom (dashed) of the target interval (bottom layer) beneath the LH layer are shown for comparison. The horizontal axis is the depth of the top of the target interval. The LH layer is located at 1 km depth with thickness $z_2 = 0.2$ km and $\partial^2\tau_{02}/\partial y_1^2 = 0.02\,(\mathrm{s/km^2})$. The velocity at the CMP location ($y_1 = 0$ km) is 3 km/s for all depths, and the thickness of the target interval is (a) 1 km and (b) 0.5 km.

3 NUMERICAL TEST

Next, we compare analytic NMO ellipses computed from equations 11 and 15 with the ellipses reconstructed from synthetic data generated with a 2D finite-difference algorithm (the code is part of the Madagascar open-source software package). The model includes an isotropic

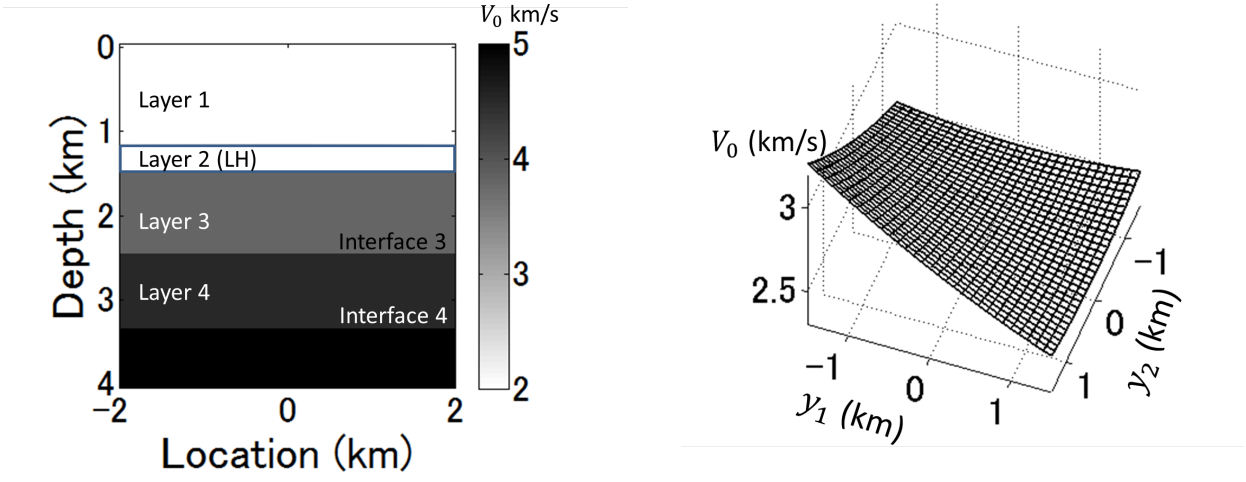

(a) (b)

Figure 5. (a) Stratified HTI model that includes an isotropic LH layer. (b) Lateral variation of the vertical velocity V_0 in the LH layer.

	Layer 1	Layer 2	Layer 3	Layer 4
V_0 (km/s)	2.0	2.5-3.2	3.8	4.5
$\delta^{(V)}$	-0.05	0	-0.03	-0.07
φ (degrees)	-45	-	-45	-45

Table 1. Parameters of the model from Figure 5. The vertical velocity V_0 in layer 2 is shown in Figure 5b. The Thomsen-style parameter $\delta^{(V)}$ is defined in the symmetry-axis plane (e.g., Tsvankin, 2005), and φ is the azimuth of the symmetry axis with respect to the axis y_1.

	Interface 3	Interface 4	Interval (Layer 4)
Analytic (%)	7.3	12	18
Numerical (%)	8.1	13	20
Background (%)	3.5	4.9	7.5

Table 2. Eccentricity of the effective NMO ellipses $W_{ij}^{\rm het}$ for interfaces 3 and 4 and that of the interval NMO ellipse for layer 4 from the model in Figure 5 and Table 1. The analytic values are computed from equation 11, and the values from numerical modeling are obtained by 3D hyperbolic semblance analysis with a spreadlength-to-depth ratio of unity. The interval NMO ellipses are found from equation 15 without correcting for lateral heterogeneity. The azimuth of the major axis of all NMO ellipses is 45°.

LH interval embedded in a layered HTI (transversely isotropic with a horizontal symmetry axis) medium (Figure 5 and Table 1). Since lateral heterogeneity and azimuthal anisotropy are weak, reflection traveltimes in any azimuthal direction are well-approximated by those computed from the 2D algorithm, as was confirmed by comparing shot gathers produced by 2D and 3D modeling. The analytic NMO ellipses $W_{ij}^{\rm het}$ are obtained using the second derivatives of the interval traveltime τ_{02} at the CMP location and the exact expression for $W_{ij}^{\rm hom}$. Since the interval traveltime surface for the LH layer from the model in Figure 5 is sufficiently smooth, the second derivatives are directly evaluated at the CMP location. The ellipses from the synthetic data are computed by the "global" semblance search using all available source-receiver pairs (Grechka and Tsvankin, 1999). The interval NMO ellipses are then obtained from the generalized Dix equation 15 without correcting for lateral heterogeneity. The difference in the eccentricity computed by the two methods is just 1% for the effective NMO ellipses and 2% for the interval ones (Table 2).

This test also confirms that the distortion caused by an LH layer in the overburden increases with reflector depth and is further amplified by the Dix equation (Table 2). The error in the interval NMO ellipse determined from the synthetic data decreases from 12.5% to 2% when the correction term is subtracted from the effective NMO ellipses (equation 11) prior to Dix differentiation (equation 15).

4 CONCLUSIONS

We presented a general analytic expression for the NMO ellipse in a stratified anisotropic medium with an arbitrary number of laterally heterogeneous (LH) layers. The equation shows that the LH-induced distortion increases with the distance between the LH interval in the overburden and the target and with the average effective NMO velocity for the target event.

Because of the depth dependence of the distortion in the effective NMO ellipses, application of the generalized Dix equation may significantly amplify the LH-related elongation or compression of the effective ellipses. To obtain an accurate interval NMO ellipse in the reference homogeneous medium, the influence of LH on the effective NMO ellipses should be removed before applying Dix differentiation. The correction for LH requires estimating the second horizontal derivatives of the interval vertical traveltime in the LH layer and the circular (isotropic) approximations of the interval NMO velocity for all layers. Synthetic tests for typical models with moderate azimuthal anisotropy and lateral heterogeneity confirm the accuracy of the developed analytic expression.

The method outlined here can be applied to layered media with multiple LH layers. To find the total LH-induced term of the NMO ellipse, it is necessary to estimate the second horizontal traveltime derivatives in all LH layers. Since the influence of weak anisotropy on the correction term is negligible, the method is applicable to lower-symmetry (orthorhombic and monoclinic) media with a horizontal symmetry plane. However, our formalism becomes inaccurate if anisotropy or lateral heterogeneity is strong, or when the model contains dipping or curved reflectors. Although the correction for LH substantially reduces the distortion in the interval moveout, Dix differentiation is sensitive to even small errors in the effective NMO ellipses, particularly when the target interval is relatively thin.

5 ACKNOWLEDGMENTS

We are grateful to M. Al-Chalabi, T. Alkhalifah, E. Blias, T. Davis, V. Grechka, E. Jenner, and W. Lynn and to members of the A(nisotropy)-Team of the Center for Wave Phenomena (CWP), Colorado School of Mines (CSM) for helpful discussions. This work was supported by Japan Oil, Gas and Metals National Corporation (JOGMEC) and the Consortium Project on Seismic Inverse Methods for Complex Structures at CWP.

REFERENCES

Blias, E., 2009, Stacking velocities in the presence of overburden velocity anomalies: Geophysical Prospecting, **57**, 323–341.

Grechka, V., and I. Tsvankin, 1998, 3-D description of normal moveout in anisotropic inhomogeneous media: Geophysics, **63**, 1079–1092.

——— 1999, 3-D moveout inversion in azimuthally anisotropic media with lateral velocity variation: Theory and a case study: Geophysics, **64**, 1202–1218.

Grechka, V., I. Tsvankin, and J. K. Cohen, 1999, Generalized Dix equation and analytic treatment of normal-moveout velocity for anisotropic media: Geophysical Prospecting, **47**, 117–148.

Jenner, E., 2009, Data example and modelling study of P-wave azimuthal anisotropy potentially caused by isotropic velocity heterogeneity: First Break, **27**, 45–50.

——— 2010, Modelling azimuthal NMO in laterally heterogeneous HTI media: First Break, **28**, 89–94.

Jenner, E., M. Williams, and T. Davis, 2001, A new method for azimuthal velocity analysis and application to a 3D survey, Weyburn field, Saskatchewan, Canada: 71th Annual International Meeting, SEG, Expanded Abstracts, 102-105.

Luo, M., M. Takanashi, K. Nakayama, and T. Ezaka, 2007, Physical modeling of overburden effects: Geophysics, **72**, no. 4, T37–T45.

Takanashi, M., and I. Tsvankin, 2010, Correction for the influence of velocity lenses on nonhyperbolic moveout inversion for VTI media: 80th Annual International Meting, SEG, Expanded Abstracts, **29**, 238–242.

——— 2011, Moveout inversion of wide-azimuth data in the presence of velocity lenses: CWP report.

Tsvankin, I., 2005, Seismic signatures and analysis of reflection data in anisotropic media, 2nd ed: Elsevier Science Publishing Company, Inc.